DOI: https://doi.org/10.14311/TPFM.2024.022

RUNGE-KUTTA DISCONTINUOUS GALERKIN METHOD APPLIED TO SHALLOW WATER EQUATIONS WITH FLOODING AND DRYING TREATMENT

C. Poussel [1], M. Ersoy [1], F. Golay [1]

[1] **Université de Toulon, IMATH, EA 2137, 83957 La Garde, France**

Abstract

This work is devoted to the numerical simulation of Shallow Water Equations involving dry areas and a moving shoreline. The space and time discretization using the Runge-Kutta Discontinuous Galerkin approach is applied to nonlinear hyperbolic Shallow Water Equations. Problems with dry areas are challenging problems for such methods. To counter this issue, special treatment is applied around the shoreline. This work compares two treatments, one based on slope modification and one based on p-adaptation.

Keywords: Discontinuous Galerkin method, Shallow Water Equations, Flooding and drying, positivity preserving.

1 Introduction

This work is developed in the framework of the interaction between the flow of water in sandy beaches and the free surface flow above the sand. Simulating the flow of groundwater has been done by Clement in 2021 [2] using the adaptive Discontinuous Galerkin method to solve Richards' equation. The present work aims to develop the hyperbolic part, in order to couple it with the parabolic one. The free surface flow over sandy beaches is modeled using the Shallow Water Equations (SWE). They are derived by considering the depth-averaged three-dimensional incompressible Navier-Stokes Equations, assuming hydrostatic pressure distribution and neglecting vertical acceleration and viscous effects [4, 12].

Discontinuous Galerkin (DG) methods were introduced in 1989 by Cockburn [3] in the scope of conservative laws. They combine the background of Finite Element methods and Finite Volume methods since the solution is sought in a broken Sobolev space, and the solution is approximated with discontinuous polynomials. Moreover, in the context of hyperbolic problems, numerical fluxes are approximated, considering the problem's physics. Due to the discontinuous approximation, the DG methods are well adapted to non-conformal meshing. As in Finite Volume methods, increasing the DG space approximation order introduces spurious oscillations of the numerical solutions. To counter this unwanted effect, slope limiting [3] and moment limiting [10] can be used. More recently, such methods were broadly used to solve SWE [7, 5]. DG methods can not natively treat flooding and drying problems due to the loss of hyperbolicity on the shoreline. Consequently, a post-processing is needed to preserve the positivity of the water height [16]. The primary purpose of this work is to implement and compare two different methods of flooding and drying treatment.

This paper is organized as follows. In Section 2, we recall the expression of SWE in two dimensions with a bathymetry source term. We detail the space discretization in Section 3. In Section 4, the fully discretized DG formulation is given with modification to ensure the well-balanced property and limit spurious oscillations. In Section 5, positivity-preserving procedures are introduced to treat the moving shoreline. In Section 6, a one-dimensional test case with a moving shoreline is presented, and a one-dimensional experimental problem with flooding and drying is solved.

2 Governing equations

Let us consider an open domain Ω, a subset of $\mathbb{R}^2$, and consider $T > 0$ as the simulation time. The gravitational acceleration is denoted by g, and $z_b : \Omega \to \mathbb{R}$ being a smooth function representing the bathymetry. The SWE system in its vectorial form is:

$$\partial_t \mathbf{U} + \operatorname{div} \mathbb{G}(\mathbf{U}) = \mathbf{S}(\mathbf{U}, z_b) \quad \text{in}\Omega\times]0, T[, \tag{1}$$

with initial and boundary conditions chosen according to the problem to be solved. In System (1) $\mathbf{U} := (h, \mathbf{q})^T : \Omega \times [0, T[\rightarrow \mathbb{R}^3$ are the conservatives variables with h the water height, $\mathbf{q} = h\mathbf{u} = (q_x, q_y)^T$ the horizontal discharge and $\mathbf{u}$ the horizontal velocity and $\mathbb{G}(\mathbf{U}) = (\mathbf{G}_1(\mathbf{U}), \mathbf{G}_2(\mathbf{U}))$ is the flux. The three equations in System (1) express mass and momentum conservation laws. They are driven by the fluxes and the source term

$$\mathbf{G}_1(\mathbf{U}) = \begin{pmatrix} q_x \\ \frac{q_x^2}{h} + g\frac{h^2}{2} \\ \frac{q_x q_y}{h} \end{pmatrix}, \mathbf{G}_2(\mathbf{U}) = \begin{pmatrix} q_y \\ \frac{q_x q_y}{h} \\ \frac{q_y^2}{h} + g\frac{h^2}{2} \end{pmatrix} \text{ and } \mathbf{S}(\mathbf{U}, z_b) = \begin{pmatrix} 0 \\ -gh\partial_x z_b \\ -gh\partial_y z_b \end{pmatrix}$$

Using the predefined variables h and z_b, the free-surface elevation ζ can be defined for all $\mathbf{x} := (x, y)$ in Ω and t in $]0, T[$, $\zeta(\mathbf{x}, t) = h(\mathbf{x}, t) + z_b(\mathbf{x})$. Figure 1 shows a sketch of the water height (h), bathymetry (z_b), and free-surface elevation (ζ) in the context of SWE.

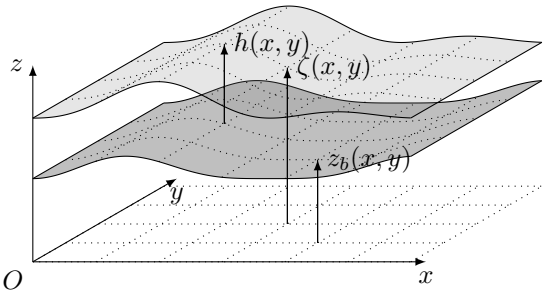

Figure 1: Sketch of the water height (h), bathymetry (z_b) and free-surface elevation (ζ) in the context of SWE.

3 Space discretization

Let us define $\mathcal{E}$ a partition of the computational domain Ω valid for all $t \in [0, T]$. For the sake of simplicity, it is assumed that Ω is a polygonal domain in two space dimensions and that $\mathcal{E}$ covers Ω exactly. The mesh $\mathcal{E}$ is composed of quadrilateral and triangular elements that are not necessarily conformal. For all elements $E \in \mathcal{E}$, d_E is its diameter defined as the ratio between its surface ($\mathfrak{s}_E$) and perimeter ($\mathfrak{p}_E$) and $d := \max_{E \in \mathcal{E}}(d_E)$.

The set of all faces of all elements $E \in \mathcal{E}$ is denoted by $\mathcal{F}$. Moreover, we can define two subsets of $\mathcal{F}$, $\mathcal{F}^\partial$ for the boundary faces and $\mathcal{F}^{\text{in}}$ for the interior faces. For a given element $E \in \mathcal{E}$, there exists a set of faces $\mathcal{F}^E := \{F \in \mathcal{F} | F \in \partial E\}$ which defines boundary of E. Then for all interior faces of E, i.e. $\forall F \in \mathcal{F}^E \cap \mathcal{F}^{\text{in}}$, there exists a neighboring element E_r such that $E \cap E_r = F$. Consequently the normal unit vector $\vec{n}_{E,F} := (n_x, n_y)^T$ pointing from E to E_r can be defined. Moreover for all boundary faces of E, i.e. $\forall F \in \mathcal{F}^E \cap \mathcal{F}^\partial$, there exists E_∂ a fictitious element such that $E \cap E_\partial = F$. Consequently, the normal unit vector $\vec{n}_{E,F}$ pointing always from E to E_∂ can be defined.

4 Fully discrete Discontinuous Galerkin Galerkin methods

This section defines the DG space and then presents the semi-discrete weak vectorial formulation. Finally, modifications are introduced to achieve the well-balanced property and limit spurious oscillations.

4.1 Discontinuous Galerkin space definition

DG methods approximate the solution within a Finite Element (FE) framework. These methods use trial and test spaces defined by piecewise polynomial functions without explicitly enforcing continuity between neighboring mesh elements. So, the first set to be defined is the set of polynomial

functions of degree $p \in \mathbb{N}$ over a mesh element E, $\mathbb{P}^p(E)$. Then, the set of piecewise polynomials functions on the mesh $\mathcal{E}$ is defined as

$$\mathcal{V}^p(\mathcal{E}) := \left\{ v : \Omega \to \mathbb{R} \;\middle|\; v_{|_E} \in \mathbb{P}^p(E),\ \forall E \in \mathcal{E} \right\}. \tag{2}$$

$\mathcal{V}^p$ is the set where the solution of System (1) is sought. It is also called the DG space. For more detailed and general definitions of the sets, see [13, chap. 1].

4.2 Semi-discrete weak vectorial formulation

By multiplying System (1) by a test function $\varphi \in \mathbb{P}^p(E)$, then by integration over Ω and finally using the divergence theorem, it gives the semi-discrete weak formulation :

$$\begin{aligned}
&\text{Find } \mathbf{U} := (h, q_x, q_y)^T \in [\mathcal{V}^p(\mathcal{E})]^3 \text{such that } \forall t \in [0,T],\ \forall E \in \mathcal{E} \text{ and } \forall \varphi \in [\mathcal{V}^p(\mathcal{E})]^3, \\
&\sum_{E\in\mathcal{E}} \int_E \varphi(\mathbf{x}) \partial_t \mathbf{U}(\mathbf{x},t) dE - \sum_{E\in\mathcal{E}} \int_E \partial_{\mathbf{x}_i} \varphi(\mathbf{x}) \mathbf{G}_i(\mathbf{U}(\mathbf{x},t)) dE \\
&+ \sum_{E\in\mathcal{E}} \sum_{F\in\mathcal{F}^E} \int_F \varphi(\mathbf{x}) \mathbf{G}_F^*(\mathbf{U}(\mathbf{x},t)) dF = \sum_{E\in\mathcal{E}} \int_E \varphi(\mathbf{x}) \mathbf{S}(\mathbf{U}(\mathbf{x},t), \tilde{z}_b(\mathbf{x})) dE
\end{aligned} \tag{3}$$

Computation of the flux at interior or boundary faces is done with $\mathbf{G}_F^*$: $\forall F \in \mathcal{F}, \forall \mathbf{x} \in F$,

$$\mathbf{G}_F^*(\mathbf{U})(\mathbf{x}) = \begin{cases} \tilde{\mathbf{G}}\Big(\mathbf{U}|_E(\mathbf{x}), \mathbf{U}|_{E_r}(\mathbf{x}), \vec{n}_{E,F} \Big), & \text{if } F \in \mathcal{F}^{\text{in}} \\ \tilde{\mathbf{G}}\Big(\mathbf{U}|_E(\mathbf{x}), \mathbf{U}|_{E_\partial}(\mathbf{x}), \vec{n}_{E,F} \Big), & \text{if } F \in \mathcal{F}^{\partial} \end{cases}$$

where $\tilde{\mathbf{G}} : \mathbb{R}^3 \times \mathbb{R}^3 \times \mathbb{R}^2 \to \mathbb{R}^3$ is the numerical flux approximation. $\mathbf{U}|_{E_\partial}$ is used to enforce boundary conditions weakly through the numerical fluxes.

This work uses the local Lax-Friedrich, also known as the Rusanov flux [8], as an approximate Riemann problem solver to evaluate $\tilde{\mathbf{G}}$ at every $F \in \mathcal{F}$. Its selection is based on its suitability for multi-dimensional hyperbolic problems, where it is easy to implement and yields good results for DG methods.

Using two-dimensional polynomial basis functions, such as tensor product Legendre basis [10] for quadrangle or the Dubiner basis [6] for triangles, the semi-discrete weak formulation can be written in a vectorial form. The solution on each element can be written as a dot product between two vectors. One holds degrees of freedom of the solution on E ($\mathbf{U}^E$), and the other holds the basis functions ($\mathbf{\Phi}$). Thus for any element $E \in \mathcal{E}$ and for all $t \in [0,T]$, it can be written as follows:

$$\forall \mathbf{x} \in E,\ \mathbf{U}(\mathbf{x},t) = \mathbf{\Phi}^T(\mathbf{x}) \mathbf{U}_E(t) \text{ and } \varphi(\mathbf{x}) = \mathbf{\Phi}(\mathbf{x})$$

Since the solution is sought in the DG space, it gives a matrix-vector system for each element. Consequently, to get the solution on Ω, one must solve System (3) for all $E \in \mathcal{E}$, for all $t \in [0,T]$ it can be written by inverting the mass matrix :

$$\text{Solve } \forall E \in \mathcal{E},\ \frac{d\mathbf{U}_E(t)}{dt} = \mathbf{H}_E(\mathbf{U}_E(t)) \tag{4}$$

where $\mathbf{H}_E : \mathbb{R}^{3N_{dof}^E} \to \mathbb{R}^{3N_{dof}^E}$. The choice of the basis is essential since it drastically affects the shape of $\mathbb{M}$; for instance, the tensor product Legendre basis makes it diagonal.

4.3 Time discretization

Numerical methods must be used to solve the ordinary differential equation in Equation (4). Only fully explicit methods will be considered here, but selecting an appropriate time step is crucial to avoid numerical instability. The explicit Euler method is the most straightforward approach, but high-order explicit Runge-Kutta (RK) algorithms are recommended for better accuracy.

The time derivative in Equation (4) is discretized using the explicit RK method of order $q = p+1$ with p the polynomial degree in $\mathcal{V}^p$. Expressions for the RK method are given in [7]. Of course, because the time discretization is explicit, the time step Δt^n is limited by the Courant-Friedrichs-Lewy (CFL) condition, which is given in [3] in the framework of Strong Stability Preserving Runge-Kutta (SSP-RK) time discretization.

4.4 Well balanced property and limiting procedure

Maintaining equilibrium states is desirable for methods handling the SWE. Specifically, we will focus on preserving *steady-states at rest*. These states are defined by the conditions $h + z_b \equiv C$ (a constant) and $\mathbf{q} \equiv 0$ over the whole domain Ω. If these conditions are not maintained, numerical waves can occur, as seen in [7]. Schemes that prevent this situation are referred to as well-balanced schemes. Unfortunately, the Runge-Kutta Discontinuous Galerkin (RKDG) scheme defined in Section 4.2 does not exhibit well-balanced properties. This is because achieving well-balancing necessitates compatibility between the numerical flux and the source term discretization. Modification of System (3) can be found in [7] to achieve well-balanced properties.

System (3) can be rewritten as a matrix-vector system for each element:

$$\text{Solve } \forall E \in \mathcal{E},\ \frac{d\mathbf{U}_E(t)}{dt} = \mathbf{H}_E^{\text{wb}}(\mathbf{U}_E(t)), \tag{5}$$

with $\mathbf{H}^{\text{wb}}$ the well balanced modified vector of the right hand side of Equation (4). $\mathbf{H}^{\text{wb}}$ has been modified according to the work of Ern [7].

When dealing with hyperbolic conservation laws, it is crucial to consider the treatment of discontinuities. High-order numerical methods may generate artificial oscillations close to discontinuities, resulting in non-physical solutions, such as negative water heights, numerical instabilities, and unbounded computational outputs.

In this work, we focus on applying the Krivodonova's [10] method on a non-conformal mesh made up of rectangular elements with Δx (Δy) denoting the length of the rectangle along the x (y) axis. However, it is worth noting that a moment limiter [6] can be applied to triangular elements, representing a generalization for non-rectangular elements. A full description of the limiting procedure can be found in [10].

Using a slope or moment limiter may affect the well-balance property. Therefore, the slope limiter should be applied to the free-surface elevation (ζ) rather than the water depth (h) to preserve the well-balanced property.

5 Flooding and drying treatment

Solving SWE can be challenging due to dry areas. Conventional approaches may fail near the dry/wet front, resulting in negative water height. Wetting and drying treatment identifies wet and dry elements and modifies the scheme to avoid negative water height. Several wetting and drying treatments are available for continuous Galerkin-based methods. One technique is the mesh adaption approach, which accurately tracks the dry front by modifying the mesh. However, this method can be computationally expensive. Secondly, the thin layer technique involves keeping a very thin layer of dry elements and incorporating them into the computation [7].

The two methods explained in the following will be based on the thin-layer approach. Nevertheless, the post-treatment applied to semi-dry elements differs for each method. The thin layer approach relies on fixing a water height threshold, h_{dry}, and using it to detect partially wet elements by looking at water height on the mesh's edges or nodes and comparing it to h_{dry}. The solution is projected to the piecewise linear space functions in a partially wet element, and the positivity-preserving method is applied.

The first method is slope modification which is the most common approach in the realm of DG methods. The second method, named $\mathbb{P}^0$-adaptation, draws inspiration from Finite Volume (FV) methods and assumes that the solution and bathymetry are piecewise constant on semi-dry elements.

5.1 Slope modification

Slope modification in DG methods was introduced by Ern in 2007 [7]. Xing in 2010 [16] improved this method. This improved method is designed to be mass and momentum-conservative with a CFL-like condition and slope modification technique. This method consists of adjusting the slope of the water height such that the water height is positive or null at nodes where the water height was negative. This slope modification is done so that the average water height is not modified. It also modifies the discharge slope of an equal factor of the water height slope.

High fluid velocity values in nearly dry regions can be observed and can cause nonphysical perturbations and lead to tiny time steps. To address this, setting a maximum value for fluid speed and discharge or setting fluid velocity to zero in shallow water depths has been suggested. A new approach involves determining the maximum velocity value based on the maximum velocity around semi-dry elements, but it can alter the solution for the given problem.

5.2 $\mathbb{P}^0$-adaptation

We can adopt a strategy similar to FV methods to handle high speeds in the shoreline area. P-adaptation is applied on element around to the shoreline, this is inspired by hp-adaptation [11] in DG methods. The solution is assumed to be piecewise constant on semi-dry elements.This approach is called $\mathbb{P}^0$-adaptation and is described as follows:

- The polynomial degree on the semi-dry element E is set to 0, preserving the average water height and discharge. It is essential to also modify the polynomial order of the bathymetry as well.

This method is mass-conservative and momentum-conservative as long as the average water height remains positive. To have this condition, the CFL-like condition in [16] needs to be used. Moreover, to be sure that potential issues due to the shoreline are avoided, one can decide to not only set semi-dry elements to $\mathbb{P}^0$ but also the elements adjacent to them in a user-defined stencil.

This method conserves mass and momentum while limiting high fluid velocities near the shoreline through numerical diffusion. It delivers reliable outcomes but can be not well-balanced in the shoreline region. The positivity-preserving technique is well-balanced in fully wet regions but can produce nonphysical perturbations in the solution at-rest state.

6 Numerical results

This section is devoted to solving test cases that are used as benchmarks for the flooding and drying treatment methods established before. This section introduces one numerical test case and one experimental test case. For conciseness, in the figures, SM denotes Slope Modification, and P0 denotes $\mathbb{P}^0$-adaptation method.

6.1 Carrier and Greenspan test case

This one-dimensional test case introduced in 1958 by Carrier and Greenspan [1] consists of a monochromatic wave running up and down on a beach plane. The solution to this problem is a periodic wave of dimensionless amplitude A^* and frequency ω^*, traveling toward the shore and being reflected out to sea, generating a standing wave on a beach plane. The analytical solution to this problem is given by [5]. The analytical solution is commonly employed to test the model's capability in handling run-up and run-down events. It is valid for $0 \leq A^* \leq 1$, and $A^*/4$ represents the maximum vertical displacement of the shoreline and $\omega^*/2$ its pulsation. The initial condition is set by providing the solution's value at $t = 0$, while the analytical surface elevation at the left boundary serves as an offshore inlet boundary condition. Variables denoted with a star are dimensionless.

In the following numerical test $A^* = 0.6$ and $\omega^* = 1$, the horizontal length scale $l = 20m$ and the slope of the beach plane is $\alpha = 1/30$. The computational domain $\Omega = [-20, 4]$ and the solution is computed util $t^* = 4T^*$. Several computations have been carried out for this test case using the following parameters: $h_{\text{dry}} = 10^{-6}$ and the stencil for $\mathbb{P}^0$-adaptation is set to 10. The mesh used is

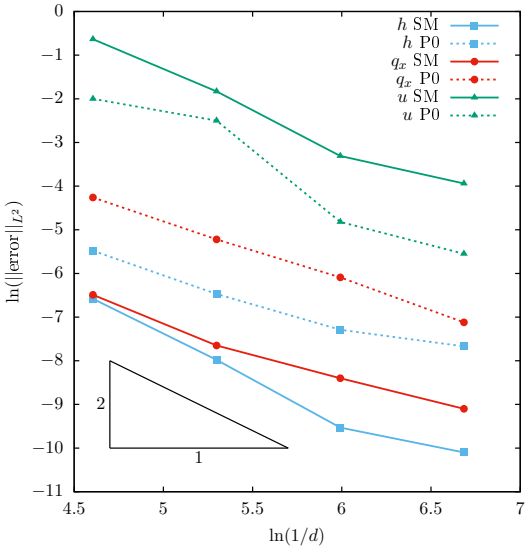

(a) Errors and convergence rates for the Carrier and Greenspan test case with different flooding and drying treatments.

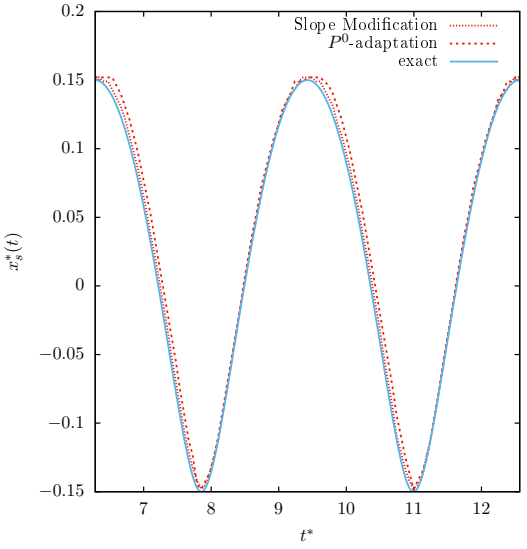

(b) Comparison of the shoreline position x_s^* computed and analytical.

Figure 2: Study of the flooding and drying treatment for the Carrier and Greenspan test case.

composed of regular one-dimensional elements of size $d = \{0.2, 0.1, 0.05, 0.025\}$, and the solution is sought in $\mathcal{V}^1$ using a RK method of order 2. Figure 2a gives the errors and convergence rates for the different flooding and drying treatments. It can be observed that convergence rates are more affected by the $\mathbb{P}^0$-adaptation method, but they are still convenient. For a smooth solution, convergence rates for a polynomial degree $p = 1$ are expected to be 2. While convergence rates for $\mathbb{P}^0$-adaptation method are greater than Slope Modification, the overall error of $\mathbb{P}^0$-adaptation for the fluid velocity are smaller. It shows that $\mathbb{P}^0$-adaptation procedure tends to diminish non-physical large fluid velocities. Figure 2b depicts the shoreline position x_s^* computed with the different flooding and drying treatments. This is extracted from previous computation with $d = 0.05m$. It compares the ability of flooding and drying treatment to recover the shoreline position. It can be observed that Slope Modification is better than $\mathbb{P}^0$-adaptation method. Moreover, one can observe that they both struggle more in the run-down phase than in the run-up phase. This is due to a better computation of the fluid velocity during the run-up than during the run-down.

6.2 Roeber test case

This test case is based on an experiment and is used to compare numerical simulations to experimental data. This test case is a problem idealized of solitary wave breaking over a two-dimensional reef. This results in a one-dimensional problem considering SWE. The geometry considered in this test case is extracted from the work of Roeber in 2010 and 2012 [15] and consists of a $83.7m$ long and $2.5m$ deep channel. The assumption of shallow water is respected. A solid wall is placed at the end of the flume. The flume's bathymetry consists of a reef with an exposed crest and a flat after the crest. The crest is $0.065m$ above the free surface, and the slope of both sides of the crest is $1/12$. The flat is $0.14m$ deep. The initial condition is a simulated solitary wave, first order solution of the Boussinesq equation with a dimensionless amplitude $A/h_0 = 0.3$ and $h_0 = 2.5m$. Variables denoted with a star are dimensionless: $\zeta^* = \zeta/h_0$ and $t^* = t\sqrt{g/h_0} + 55.3$.

Computation of the solution of this test case is done on a mesh composed of regular one-dimensional elements of size $d = 0.4185$, and the solution is sought in $\mathcal{V}^1$ using a RK method of order 2. The two flooding and drying treatments are used but with a different parameter h_{dry}. With the Slope Modification method $h_{\text{dry}} = 10^{-3}$ and with the $\mathbb{P}^0$-adaptation method $h_{\text{dry}} = 10^{-6}$ with a stencil of 10 elements. h_{dry} has to be different because the Slope Modification method produced large fluid velocity, making the time step too small and producing non-physical results.

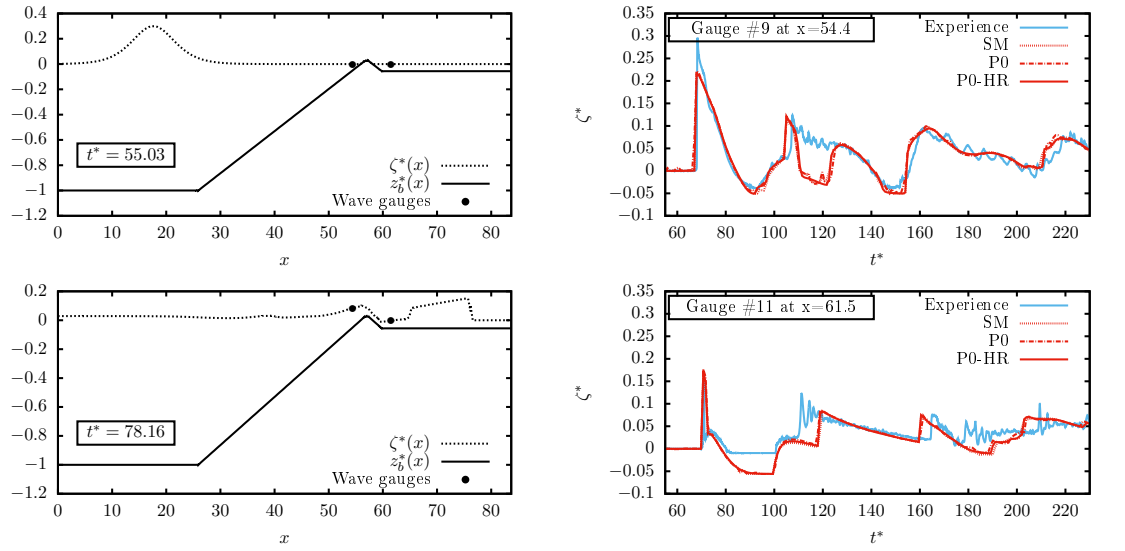

(a) Solution at two different times with Slope Modification method.

(b) Comparison of numerical solutions with experimental data with different flooding and drying method.

Figure 3: Numerical solution of the Roeber test case with different flooding and drying treatment.

Moreover, another computation is done with $d = 0.04185$, and the solution is sought in $\mathcal{V}^0$. This is a reference numerical solution for this experimental test case. Figure 3a depicts the solution at two different times, the initial condition $t^* = 55.03$ and after the breaking of the wave at $t^* = 78.16$. Figure 3b compares the numerical solution with experimental data. It can be observed that both flooding and drying methods are in good agreement with the experiment for the main event: the wave breaking over the reef. However, for events after the breaking, the numerical solution shows differences, especially for the gauge placed after the crest. There is a delay in events and a significant underestimation at $t^* \approx 90$. These discrepancies are also effective in the reference numerical solution (P0-HR) and in the work of [14] but are solved using a Boussinesq-type model in [15]. Thus, it can be considered that SWE fails to capture specific events, but the numerical method is validated.

7 Conclusion

In this paper, SWE with dry areas and bathymetry are numerically solved using a Rung-Kutta Discontinuous Galerkin method modified to be well-balanced and Total Variations Diminishing. Nevertheless, the ability to solve problems with dry areas is not straightforward for such a method. Thus, two ways to treat flooding and drying areas are introduced and implemented. one based on slope modification and the other based on p-adaptation. In order to validate the numerical simulation of SWE with dry areas, two benchmarks are passed. The first is a one-dimensional test case with an analytical solution, and the second is an experimental test case. The established numerical scheme can solve problems with dry areas with good accuracy and preserve convergence orders.

Acknowledgment

This work has been supported financially by *Provence-Alpes-Côte d'Azur region (France)*.

References

[1] Carrier, G. F. & Greenspan, H. P.: Water waves of finite amplitude on a sloping beach. *Journal of Fluid Mechanics*, vol. 4, no. 1: (1958) pp. 97–109.

[2] Clément, J-B., Golay, F., Ersoy, M. & Sous, D. : An adaptive strategy for discontinuous Galerkin simulations of Richards' equation: Application to multi-materials dam wetting. *Advances in Water Resources*, vol. 151: (2021) p. 103897.

[3] Cockburn,B. & Shu,C-W.: TVB Runge-Kutta Local Projection Discontinuous Galerkin Finite Element Method for Conservation Laws II: General Framework. *Mathematics of Computation*, vol. 52, no. 186: (1989) pp. 411–435.

[4] De Saint-Venant, A.J.C.B.: *Théorie Du Mouvement Non Permanent Des Eaux, Avec Application Aux Crues Des Rivières et à l'introduction Des Marées Dans Leur Lit.* Comptes Rendus Hebdomadaires Des Séances de l'Académie Des Sciences. Gauthier-Villars, (1871).

[5] Duran, A.: Numerical Simulation of Depth-Averaged Flow Models : A Class of Finite Volume and Discontinuous Galerkin Approaches. *Theses, Université Montpellier II*, (2014).

[6] Dutt, K. & Krivodonova, L.: A high-order moment limiter for the discontinuous Galerkin method on triangular meshes. *Journal of Computational Physics*, vol. 433: (2021) p. 110188.

[7] Ern, A., Piperno S. & Djadel, K.: A well-balanced Runge–Kutta discontinuous Galerkin method for the shallow-water equations with flooding and drying. *International Journal for Numerical Methods in Fluids*, vol. 58, no. 1: (2007) pp. 1–25.

[8] Gallouët, T., Hérard, J-M. & Seguin, N.: Some approximate Godunov schemes to compute shallow-water equations with topography. *Computers and Fluids*, vol. 32, no. 4: (2003) pp. 479–513.

[9] Gottlieb, S., Shu, C-W. & Tadmor, E.: Strong Stability-Preserving High-Order Time Discretization Methods. *SIAM Review*, vol. 43, no. 1: (2001) pp. 89–112.

[10] Krivodonova, L.: Limiters for high-order discontinuous Galerkin methods. *Journal of Computational Physics*, vol. 226, no. 1: (2007) pp. 879–896.

[11] Kubatko, E. J., Bunya, S., Dawson, C. & Westerink, J. J.: Dynamic p-adaptive Runge–Kutta discontinuous Galerkin methods for the shallow water equations. *Computer Methods in Applied Mechanics and Engineering*, vol. 198, no. 21: (2009) pp. 1766–1774.

[12] Marche, F.: Derivation of a new two-dimensional viscous shallow water model with varying topography, bottom friction and capillary effects. *European Journal of Mechanics - B/Fluids*, vol. 26, no. 1: (2007) pp. 49–63.

[13] Di Pietro, D. A. & Ern, A.: Mathematical Aspects of Discontinuous Galerkin Methods. *Springer Berlin Heidelberg*, (2012).

[14] Pons, K., Ersoy, M., Golay, F. & Marcer, R.: Adaptive mesh refinement method. Part 2: Application to tsunamis propagation. *Preprint available on hal* `https://hal.science/hal-01330680`, (2016)

[15] Roeber, V., Cheung, K. F. & Kobayashi, M. H.: Shock-capturing Boussinesq-type model for nearshore wave processes. *Coastal Engineering*, vol. 57, no. 4: (2010) pp. 407–423.

[16] Xing, Y., Zhang, X. & Shu, C-W.: Positivity-preserving high order well-balanced discontinuous Galerkin methods for the shallow water equations. *Advances in Water Resources*, vol. 33, no. 12: (2010) pp. 1476–1493.